Behavioral/Systems/Cognitive

SIRT1 Is Essential for Normal Cognitive Function and Synaptic Plasticity

Shaday Michán,[1,3]* **Ying Li,**[4,5]* **Maggie Meng-Hsiu Chou,**[4] **Edoardo Parrella,**[5] **Huanying Ge,**[6] **Jeffrey M. Long,**[7] **Joanne S. Allard,**[7] **Kaitlyn Lewis,**[7] **Marshall Miller,**[7] **Wei Xu,**[4] **Ronald F. Mervis,**[8,9] **Jing Chen,**[2] **Karen I. Guerin,**[2] **Lois E. H. Smith,**[2] **Michael W. McBurney,**[10] **David A. Sinclair,**[1] **Michel Baudry,**[4] **Rafael de Cabo,**[7] **and Valter D. Longo**[4,5]

[1]Paul F. Glenn Laboratories, Department of Pathology, Harvard Medical School and [2]Department of Ophthalmology, Children's Hospital, Harvard Medical School, Boston, Massachusetts 02115, [3]Instituto de Geriatría, Institutos Nacionales de Salud, 04510 México D.F., México, [4]Neuroscience Program, [5]Andrus Gerontology Center and Department of Biological Sciences, and [6]Molecular and Computational Biology, Department of Biology Sciences, University of Southern California, Los Angeles, California 90089, [7]Laboratory of Experimental Gerontology, National Institute on Aging, National Institutes of Health, Baltimore, Maryland 21224, [8]Center of Excellence in Aging and Brain Repair, Department of Neurosurgery and Brain Repair, University of South Florida College of Medicine, Tampa, Florida 33612, [9]NeuroStructural Research Labs Inc., Tampa, Florida 33137, and [10]Ottawa Health Research Institute, Department of Medicine, University of Ottawa, Ottawa, Ontario K1H 8M5, Canada

Conservation of normal cognitive functions relies on the proper performance of the nervous system at the cellular and molecular level. The mammalian nicotinamide-adenine dinucleotide-dependent deacetylase SIRT1 impacts different processes potentially involved in the maintenance of brain integrity, such as chromatin remodeling, DNA repair, cell survival, and neurogenesis. Here we show that SIRT1 is expressed in neurons of the hippocampus, a key structure in learning and memory. Using a combination of behavioral and electrophysiological paradigms, we analyzed the effects of SIRT1 deficiency and overexpression on mouse learning and memory as well as on synaptic plasticity. We demonstrated that the absence of SIRT1 impaired cognitive abilities, including immediate memory, classical conditioning, and spatial learning. In addition, we found that the cognitive deficits in SIRT1 knock-out (KO) mice were associated with defects in synaptic plasticity without alterations in basal synaptic transmission or NMDA receptor function. Brains of SIRT1-KO mice exhibited normal morphology and dendritic spine structure but displayed a decrease in dendritic branching, branch length, and complexity of neuronal dendritic arbors. Also, a decrease in extracellular signal-regulated kinase 1/2 phosphorylation and altered expression of hippocampal genes involved in synaptic function, lipid metabolism, and myelination were detected in SIRT1-KO mice. In contrast, mice with high levels of SIRT1 expression in brain exhibited regular synaptic plasticity and memory. We conclude that SIRT1 is indispensable for normal learning, memory, and synaptic plasticity in mice.

Introduction

Sir2, the yeast ortholog of mammalian SIRT1, was first identified as a nicotinamide-adenine dinucleotide (NAD$^+$)-dependent histone deacetylase (HDAC) that extended replicative lifespan (Kaeberlein et al., 1999). In mammals, SIRT1 orchestrates diverse biological processes, including cell differentiation (Fulco et al.,

2008), apoptosis (Luo et al., 2001), autophagy (Lee et al., 2008), development (Cheng et al., 2003), cancer (Kim et al., 2008), metabolism (Picard et al., 2004; Li et al., 2007), and circadian rhythms (Asher et al., 2008). SIRT1 modulates these functions by deacetylating a variety of substrates, including histones, enzymes, transcription factors, and critical components of signal transduction cascades (Michan and Sinclair, 2007).

Accumulating evidence suggests that SIRT1 plays critical roles in several brain functions. SIRT1 protein levels decrease in the cortex of SAMP8 (senescence-accelerated prone mice) over the course of aging and in human Huntington's disease compared with the control strain SAMR1 (senescence-accelerated resistant mice) or age-matched healthy humans (Pallàs et al., 2008), respectively. SIRT1 also regulates neuronal differentiation (Hisahara et al., 2008; Prozorovski et al., 2008), participates in neuronal protection by ischemic preconditioning in hippocampus (Raval et al., 2008), and prevents neurodegeneration in mouse models of neuronal diseases, including amyotrophic lateral sclerosis (Kim et al., 2007) and Alzheimer's disease (Chen et al., 2005; Qin et al., 2006). In neurons, SIRT1 prevents mitochondrial loss elicited by mutant α-synuclein or mutant huntingtin

(Wareski et al., 2009) and modulates DNA damage response (Hasegawa and Yoshikawa, 2008). Furthermore, SIRT1 is regulated by energy availability in hypothalamus (Ramadori et al., 2008), and it is importantly involved in the regulation of the somatotropic axis (Cohen et al., 2009). Also, SIRT1 together with SIRT2 participates in the cocaine rewarding effect regulated by the nucleus accumbens (Renthal et al., 2009). However, the role of SIRT1 is not straightforward because SIRT1 inhibition protects cultured cortical neurons against oxidative stress (Li et al., 2008).

Regulation of gene expression through histone acetylation is an essential component of learning and memory (Fischer et al., 2007). Long-term potentiation (LTP), an experimental form of synaptic plasticity and a major cellular mechanism underlying learning and memory, is enhanced by histone acetylation (Levenson et al., 2004a). Notably, SIRT1 regulates chromatin remodeling and histone acetylation (Vaquero et al., 2004). Likewise, the activity of transcription factors such as nuclear factor-κB (Meffert et al., 2003; Yeung et al., 2004; Ahn et al., 2008) and myocyte enhancer factor 2 (Zhao et al., 2005; Barbosa et al., 2008), as well as the insulin/IGF-1 and insulin receptor substrate-2 (IRS-2)/extracellular signal-regulated kinase 1 (ERK1) signaling pathways, which play important roles in cognition, are also modulated by SIRT1 (Lemieux et al., 2005; Li et al., 2008).

Although different studies suggest that SIRT1 is involved in neuropathology, the role of this protein in normal cognitive functions is not clear. In this study, we show that SIRT1 is expressed in neurons of the hippocampus, a critical structure for learning and memory. We found that SIRT1 knock-out (KO) mice exhibited a significant deficit in both short- and long-term hippocampus-dependent memory. Interestingly, the cognitive impairment was associated with decreased LTP in hippocampal field CA1 without alterations in NMDA receptor function, basal synaptic properties or dendritic spine architecture. However, neurons from SIRT1-KO mice showed less dendritic branching and decreased branch length and complexity of neuronal dendritic trees. Also, SIRT1 knock-out mice exhibited differential hippocampal gene expression and decreased ERK1/2 phosphorylation. In contrast, mice expressing high levels of SIRT1 in hippocampus showed normal LTP and memory. Our data led us to conclude that SIRT1 is essential for mouse normal cognitive function but that its overexpression does not modify learning and memory.

Materials and Methods

Animals. SIRT1-KO (McBurney et al., 2003) and NeSTO mice (Oberdoerffer et al., 2008) were pathogen free housed in ventilated cages on a 12 h light/dark cycle at 22°C and 35% humidity with *ad libitum* access to food and water. All testing was performed during the light phase of the cycle.

Nissl staining, immunohistochemistry, and Western blotting. SIRT1 wild-type (WT) and KO brains were perfused with 4% formaldehyde, postfixed for 2 h, and sucrose cryoprotected for 15 h. Coronal sections (30 μm) were stained with cresyl violet for Nissl staining or antigen retrieved for immunostaining. Mouse SIRT1 at 1:1000 (Millipore), neuronal-specific nuclear protein (NeuN) at 1:500 (Millipore), or glial fibrillary acidic protein (GFAP) at 1:500 (Sigma) antibodies were used as primary antibodies, and Alexa Fluor-488 and Alexa Fluor-568 at 1:500 (Invitrogen) were used as secondary antibodies. Half brains from NeSTO and Nestin–Cre mice were fixed for 24–48 h in 4% formaldehyde and paraffin embedded, and 5-μm-thick coronal sections were cut. Slices were deparaffinized, rehydrated, and microwave irradiated for antigen retrieval. Sections were incubated with primary antibodies overnight at 4°C. *Z*-stacks were obtained with an Olympus confocal microscope using

Kalman filter and sequential scanning mode. For immunoblotting, proteins from hippocampal lysates were separated by SDS-PAGE and electrotransferred to a polyvinylidene difluoride membrane. An anti-mouse SIRT1 polyclonal antibody (Millipore) was used for immunoblotting, and results were quantified using the ImageQuant software.

Open field. A gray Plexiglas (49 cm length × 49 cm width × 40 cm height) wood-stick bedded box was used as the open-field arena. Mice were handled for 6 d, followed by 3 d of habituation to the open-field arena (30 min the first day and 15 min the next 2 d). On the day of testing, animals were placed in the center of the arena and left to explore it for 30 min while activity was automatically recorded with a video tracking system (VideoMot2; TSE Systems).

Y-maze test. The Y maze was a three-arm maze, made of black Plexiglas with equal angles between all arms. Two- to 5-month-old mice were individually tested by placing them within one arm of the maze and allowing them to move freely throughout the three different arms of the maze over an 8 min period. The sequence and entries in each arm were recorded, and alternation was determined from successive consecutive entries to the three different arms on overlapping triads in which all arms were represented. For example, a sequence of entries to the three arms ABC, ACBABCABAB, would generate five "successful" alternations, ACB, CBA, ABC, BCA, and CAB; the total number of possible alternations corresponded to the number of arm entries minus two (for this example, total number would equal eight). The percentage of alternations per total entries was then calculated (Hughes, 2004).

Novel object recognition test. Two pairs of identical objects were alternatively used for this experiment. One pair was placed in the wood-stick bedded open-field arena described above. Habituated mice were placed in the arena and left to interact with the pair of objects for 15 min. Mice were placed back in their cages and left rest for 1.5 h. Afterward, one of the familiar objects was replaced by a novel object, and animals were allowed to explore the arena for 5 min. Object interaction was automatically recorded with a video tracking system (VideoMot2; TSE Systems). Discrimination index was calculated as the proportion of time the animals explored the novel object minus the proportion exploring the familiar object during the testing period.

Fear conditioning. Five- to 10-month-old mice were trained in the conditioning chamber. After a 3 min baseline period, three tone–footshock pairings (tone, 20 s, 80 dB, 2 kHz; footshock, 1 s, 0.8 mA) separated by 1 min intervals were delivered. Contextual fear conditioning was assessed 24 h after training by placing back the mouse in the same test chamber for 5 min. Freezing to altered context was tested in a novel chamber 48 h after training for 3 min. Afterward in this second chamber, the training tone was delivered for 5 min to evaluate tone conditioning. Freezing behavior, defined as the absence of all visible movement of the body, except from movement necessitated by respiration, was scored and expressed as percentage of the observation period.

Barnes maze. The maze consisted of a white platform (91 cm in diameter, 91 cm height) with 20 holes (5 cm in diameter) located 2.5 cm from the perimeter (San Diego Instruments) (Barnes, 1979). A black escape box (EB) was placed under one of the holes, and 19 false target boxes were placed under all other holes. Two-month-old mice were brought into the testing room 1 h before the experiment. Each mouse was randomly assigned a unique position for the EB, and it was always located underneath the same hole for a particular mouse. All mice were trained once daily from day 0 to 7 and tested twice daily from day 1 to 7. During training sessions, the mouse was placed in the middle of the maze in a start chamber for 30 s and then allowed to freely explore the maze until either entering the EB or after 2 min elapsed. Once mouse entered the EB, it was left there for 30 s. If the mouse did not enter the EB by itself, it was gently guided to and allowed to stay in the EB for 30 s. After the training session, mice were tested twice daily for 7 d. Testing was similar to training, but if after 2 min the mouse did not find the escape box, it was directly returned to its home cage. Latency (the time taken to enter the EB), number of errors (defined as nose pokes and head deflections over any false target hole), deviation of the first error (how many holes away from the EB was the first error), and strategy used by the mouse to locate
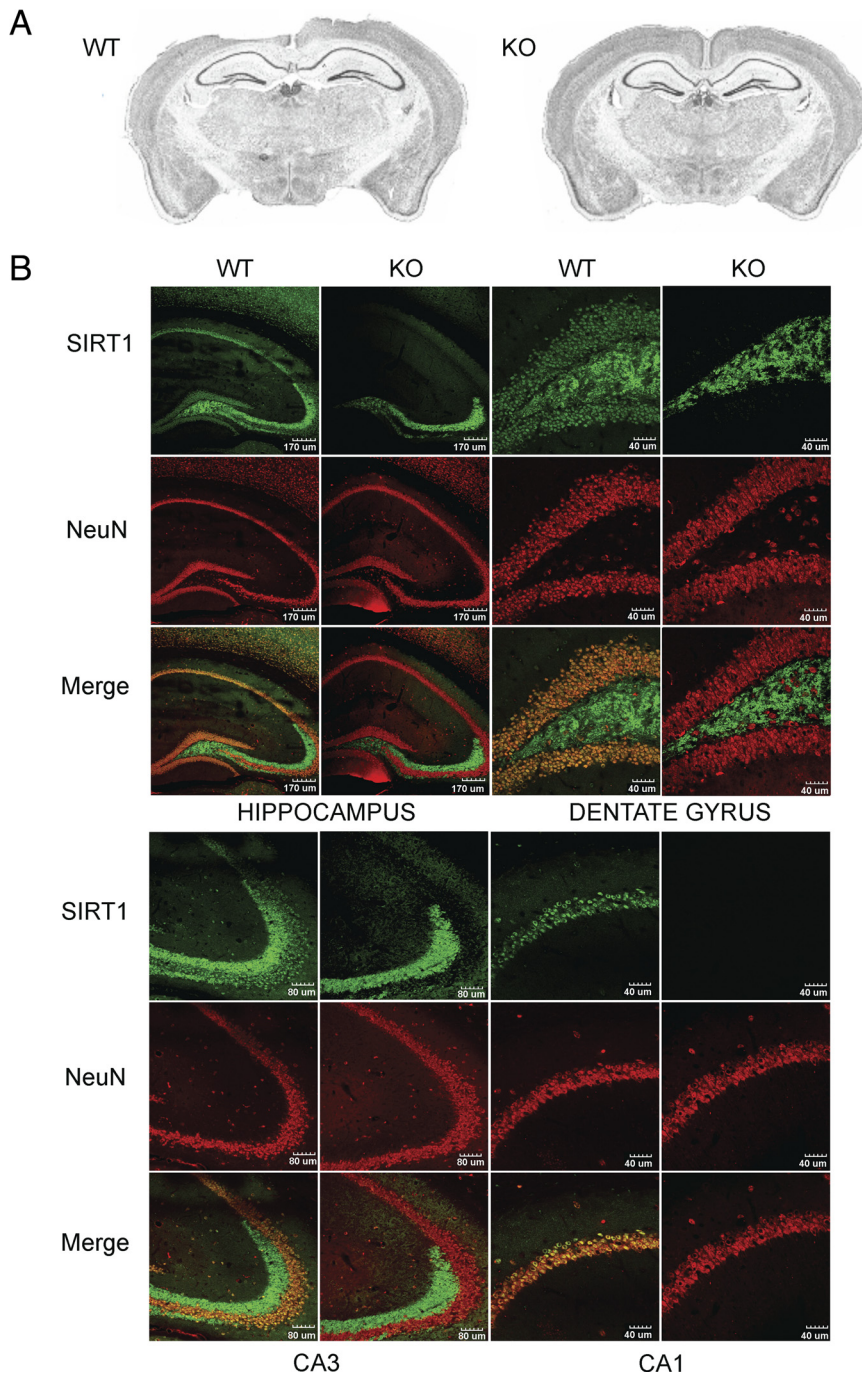
Figure 1. Absence of SIRT1 in hippocampal neurons of knock-out mice does not impact normal gross brain anatomy. **A**, Representative images of SIRT1-KO and WT Nissl-stained coronal brain sections. SIRT1-KO brains show normal gross neuroanatomy. **B**, Immunofluorescence of coronal brain sections from SIRT1-KO and WT mice. SIRT1 and NeuN are colocalized in WT hippocampal neurons in different areas, including the dentate gyrus, CA1, and CA3. SIRT1-KO sections show absence of SIRT1 in hippocampal neurons yet unaltered NeuN staining.

Vision test. Pupillary reflexes were examined by shining a bright light into the eye. To test visual perception, a black bar was inserted quickly into the home cage, and mouse escape behavior was examined. Also, we used the visual placing test in which the mouse was held by its tail at a height of ~15 cm from a table surface. As the mouse was gradually lowered, extension of its forepaws for a "soft landing" in the horizontal surface was observed. We further tested mice vision in a cue test in the water maze. Habituated mice were allowed to swim to complete four trials per day during 2 d with a visible platform marked with a flag. Initial position of the mouse and the platform were changed in each trial, and latency was automatically recorded with a video tracking system (VideoMot2; TSE Systems).

Eye morphology. The eyes of SIRT1-KO and WT mice were examined in live animals for cataract and other abnormality. For retinal sections, eyes isolated from SIRT1-KO and WT control mice were fixed in 4% paraformaldehyde and frozen in OCT. Fourteen-micrometer-thick sections were mounted on slides, rinsed with PBS, and stained with hematoxylin and eosin by standard methods for general morphology. For immunohistochemistry, retinal sections were blocked in PBS with 0.1% Triton X-100 and 5% bovine serum albumin. Sections were incubated overnight with *Griffonia Bandeiraea simplicifolia* isolectin B4 conjugated with Alexa Fluor-594 (catalog #I21413; Invitrogen) and primary antibodies against GFAP (1:500; catalog #ab7260; Abcam), followed by anti-rabbit secondary antibodies conjugated with Alexa Fluor-488 (1:200; catalog #A11034; Invitrogen) and counterstained with 4′,6′-diamidino-2-phenylindole (DAPI) (catalog #H-1200; Vector Laboratories). Images were taken with a fluorescence microscope (Axio Observer Z1; Carl Zeiss).

Hippocampal slices preparation. Mice at 3–4 months of age (SIRT1-KO and WT) or 9–12 months of age (Nestin–Cre and NeSTO) were anesthetized with halothane and decapitated. Brains were quickly removed and transferred to oxygenated, ice-cold, high-magnesium artificial CSF (ACSF) cutting medium (in mM: 124 NaCl, 26 NaHCO$_3$, 10 glucose, 3 KCl, 1.25 KH$_2$PO$_4$, 5 MgSO$_4$, and 3.4 CaCl$_2$). Hippocampal transversal slices (400-μm-thick) were made using a McIlwain-type tissue chopper and maintained for 40 min in a recovery chamber with oxygenated ACSF at room temperature. Slices were then transferred to an interface recording chamber and exposed to a warm, humidified atmosphere of 95% O$_2$/5% CO$_2$ with preheated (33 ± 0.5°C) oxygenated ACSF perfused at 1 ml/min.

Field recording. After a minimum of 1 h incubation in the recording chamber, a single glass pipette filled with normal ACSF (yielding a resistance of 3–5 MΩ) was used to record field EPSPs (fEPSPs) with twisted nichrome wires (single bare wire diameter, 50 μm). Before each experiment, the input/output (I/O) relations was examined, and the stimulation intensity was adjusted to obtain 40–50% of the maximum fEPSP amplitude without spike component in the response. The adjusted stimuli (test pulses) were then delivered at 0.05 Hz, and responses were recorded. After establishing a 10 min stable baseline, LTP was induced by

the EB were recorded for each testing. Search strategies were classified as random (localized hole searches separated by crossings through the maze center), serial (systematic hole searches in a clockwise or counterclockwise direction), or spatial (navigating directly to the EB with both error and deviation scores of no more than 3). Success rate for each test was either 100% (finding the EB within 2 min) or zero (not finding the EB within 2 min). For mice that did not find the EB within 2 min, the latency was scored as 120 s (Bach et al., 1995). All measures were averaged from two tests to obtain each mouse daily value. Retention was assessed by testing each mouse once on day 14.

using two different protocols (supplemental Fig. 2A, available at www.jneurosci.org as supplemental material). Paired-pulse facilitation (PPF) responses were examined on different slices than those used for LTP. Five different interpulse intervals were tested: 30, 50, 100, 200, and 300 ms. Data were collected and digitized by NAC 2.0 Neurodata Acquisition System (Theta Burst Inc.). Each fEPSP was analyzed for its initial falling slope. PPF of fEPSP amplitude was obtained from the following calculation: PPF = [(second fEPSP − first fEPSP)/first fEPSP] × 100%.

Dendritic analysis. Seven-month-old brains were fixed in 10% Formalin, and coronal tissue blocks were dissected out, which encompassed the parietal cortex and the underlying hippocampus. Tissue was stained using the rapid Golgi method (Valverde, 1976). In this technique, the dendritic arbor and soma of ∼5% of all neurons are randomly impregnated with a silver chromate precipitate. The blocks were dehydrated, and the tissue blocks were then subsequently embedded in nitrocellulose and sectioned at 120 μm thickness. Sections were cleared in α-terpineol, rinsed in xylene, and coverslipped under Permount. All brains were re-coded, and the studies were performed blind as to group or paradigm.

Analysis of dendritic spines was performed on the apical tree of hippocampal CA1 pyramidal neurons of stratum radiatum. Spines were counted along segments at various distances from the soma. In addition to spine density (e.g., spines per segment length), spines were also evaluated in terms of spine configuration or morphology. From each brain, spines from five CA1 neurons were evaluated. Only spines from CA1 pyramidal neurons of hippocampus that were well stained and whose branches were not obscured by other CA1 dendrites, blood vessels, or nondescript precipitates were quantified. Spine density and morphology were counted along three terminal tip segments from each neuron. All visible flanking spines were counted along terminal tip segments of a variable length (usually 20–30 μm long). This exact segment distance was measured using a digitizing tablet, and spine density (spines per unit length) was calculated. The distances of the analyzed segments from the soma were also measured. Granule cells of both upper and lower blades of hippocampal dentate gyrus were randomly selected for dendritic branching analysis. Camera lucida drawings of the dendritic branches of the selected neurons were prepared and examined using Sholl analysis. Statistical significance was evaluated using different tests, including the unpaired Student's *t* test, Wilcoxon's signed rank test, and Mann–Whitney test.

Microarray analysis. Hippocampi were carefully dissected, and total RNA was isolated with Trizol reagent (Invitrogen). For Affymetrix expression analysis, total RNA was hybridized to the mouse genome 430 2.0 array. CEL files were analyzed for significance and fold changes between experimental groups with the statistical software R using the Affymetrix package (Gautier et al., 2004). The microarray data were processed using the invariant-set normalization (Li and Hung Wong, 2001), followed by the model-based (model-based expression index) summarization (Li and Wong, 2001) to obtain expression for each probe set.

Statistical analysis. Y-maze and fear conditioning data were analyzed by Student's *t* test. For Barnes maze, rotarod, and open-field data,
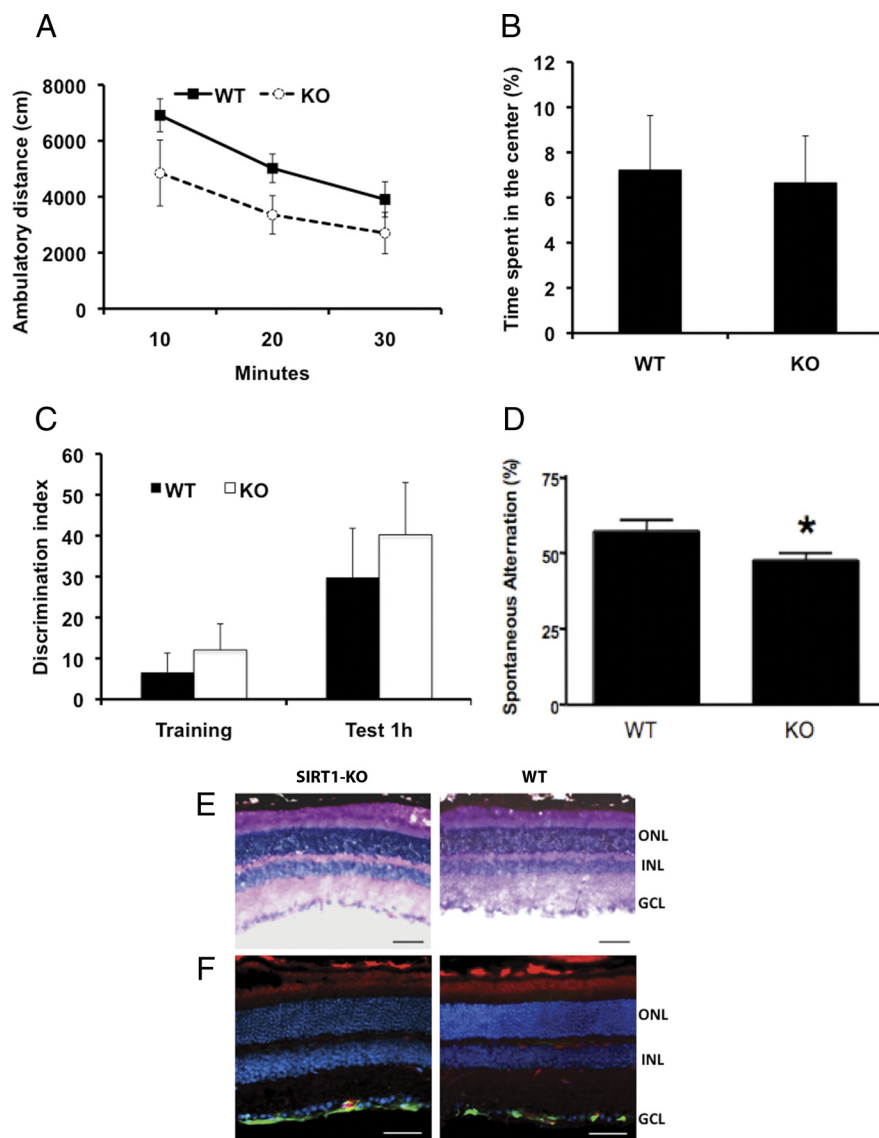

Figure 2. The lack of SIRT1 does not affect exploratory behavior but leads to deficits in immediate memory. *A*, *B*, SIRT1-KO mice showed normal exploratory behavior in the open field compared with WT as revealed by distance traveled (*A*) and time spent in the center of the arena (*B*) ($n = 4$ per genotype; WT, 3.6 ± 1.05%; KO, 3.4 ± 1.5%). *C*, Novel object recognition test shows normal discriminatory ability to a novel object in SIRT1-KO mice ($n = 4$ per genotype; training WT, 7 ± 5; training KO, 12 ± 6; test WT, 30 ± 12; KO test, 40 ± 13; $p > 0.5$). *D*, Decreased spontaneous alternation in the Y maze compared with WT mice ($n = 16$ per genotype; WT 58 ± 4 vs KO 48 ± 2%; *$p < 0.05$). Data represent means ± SEM. *E*, Cross sections of retinas from SIRT1-KO and WT mice show normal morphology of all retinal layers (ONL, outer nuclear layer; INL, inner nuclear layer; GCL, ganglion cell layer) by hematoxylin and eosin staining as well as by isolectin (red), GFAP (green), and DAPI (blue) staining (*F*). Scale bars, 100 μM.

ANOVA was used with *post hoc* analysis. For the water maze data, a two-way or a two-way with repeated measures ANOVA followed by a Fisher's protected least significant difference test were used. For electrophysiological data, each slice was considered as an individual *n*. Statistical significance was assessed by either two-way ANOVA or two-tailed unpaired Student's *t* test. An α level of 0.05 was used as the criterion for significance for all analyses.

Results

SIRT1 localizes in neurons important for cognition

To investigate the role of SIRT1 in learning and memory, we first examined brain histology in WT and SIRT1-KO mice (McBurney et al., 2003). No discernable gross neuroanatomical differences were observed by Nissl staining (Fig. 1A) or immunohistochemistry with the neuronal marker NeuN (Fig. 1B). To determine

whether endogenous SIRT1 was expressed in brain areas important for cognitive functions, we studied its distribution in brain sections using a mouse-specific anti-SIRT1 antibody. In WT mice, SIRT1 was colocalized with NeuN and DAPI staining but not with the glial marker GFAP throughout the hippocampus, including the granule neurons in dentate gyrus and the pyramidal neurons in CA3 and CA1 areas (Fig. 1 B) (supplemental Fig. S4, available at www.jneurosci.org as supplemental material). The absence of fluorescence in hippocampal neurons of SIRT1-KO mice confirmed that the antibody specifically recognizes SIRT1. Nonspecific labeling was detected in the mossy fibers, as observed previously with other antibodies. Our data indicate that SIRT1 is highly expressed in brain areas that play crucial roles in memory formation and normal cognitive performance and that gross neuroanatomy is not impacted by the lack of SIRT1.

SIRT1 knock-out mice show defects in immediate memory
First, we tested SIRT1-KO mice in the open field to examine locomotor activity and exploratory behavior. During 30 min of exploration, SIRT1-KO mice traveled similar distance as WT mice (Fig. 2 A) and spent equal time in the center of the arena, showing no differences in exploratory behavior (Fig. 2 B). To assess the effect of SIRT1 in cognition, we tested short-term memory of SIRT1-KO mice in the Y maze. Animals were allowed to move freely in the maze, and spontaneous alternation (SA) behavior was determined by examining the sequence of visits to all three arms on consecutive choices. A high rate of alternation reflects a higher capacity to discern which arm was entered last. In this paradigm, SIRT1-KO mice exhibited a moderate but significantly lower SA than WT mice (Fig. 2 D) despite higher total entries (supplemental Fig. S1 A, available at www.jneurosci.org as supplemental material). Gender analysis also revealed a significant SA decrease in KO males (supplemental Fig. S1 B, available at www.jneurosci.org as supplemental material), whereas the number of entries was similar to that of WT mice (supplemental Fig. S1 C, available at www.jneurosci.org as supplemental material). However, no differences were detected between female genotypes, although KO females were more active than WT females (supplemental Fig. S1 B, C, available at www.jneurosci.org as supplemental material). Also, both strains had similar object exploratory behavior during training in the novel object recognition test (NORT) (Ennaceur et al., 1997) and equivalent discriminatory capacity when a novel object was replaced by a familiar object, showing that conservation of short-term object recognition memory in SIRT1-KO female mice was not affected (Fig. 2 C).

In addition, we analyzed pupillary reflex and visual perception (see Material and Methods) and found no differences between genotypes (data not shown). Furthermore, a detailed examination showed that isolated eyes from both groups had comparable size, the lenses were clear with no visible signs of opacity or structural alteration, and retinal cross sections also revealed normal morphology of neurons and blood vessels with comparable retina thickness (Fig. 2 E). Similarly, GFAP staining in retinas of SIRT1-KO and WT mice indicated absence of retinal injury or stress in the eyes of both groups of mice (Fig. 2 F). Together, these data demonstrate that SIRT1-KO mice have an intact eye structure and visual perception.

Lack of SIRT1 impairs short-term and long-term associative memory
We next used the classical Pavlovian paradigm of fear conditioning to assess associative memory. In this task, mice learn to associate an emotionally neutral conditioned stimulus such as an
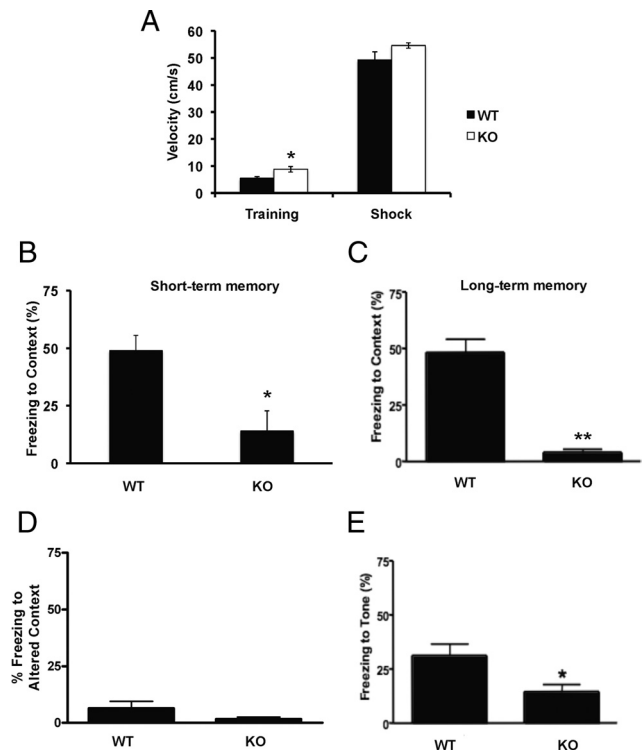

Figure 3. SIRT-KO mice are markedly impaired in associative memory. **A**, SIRT1-KO mice show slightly higher activity ($n = 4$ per genotype; WT, 5.5 ± 0.6 cm/s; KO, 8 ± 1.2 cm/s; *$p < 0.05$) yet similar responses to electric shock than WT mice during training. **B**, **C**, Conditioning to context short term (**B**) ($n = 4$ per genotype; WT, $49 \pm 7\%$; KO, $14 \pm 9\%$; *$p < 0.05$) and long term (**C**) (WT, $n = 13$, $48 \pm 6\%$; KO, $n = 10$, $4 \pm 1.5\%$; **$p < 0.001$). **D**, Freezing to altered context did not reveal differences between genotypes (WT, $n = 13$; KO, $n = 10$). In contrast to SIRT1-KO, wild-type mice show significantly decreased fear responses in the altered context compared with that in the training context (6 ± 3 vs $48 \pm 6\%$, respectively; $p < 0.001$). **E**, In conditioning to tone, SIRT1-KO mice ($n = 10$; $14 \pm 4\%$) also displayed decreased performance compared with WT mice ($n = 13$; $31 \pm 6\%$; *$p < 0.05$). Data represent means ± SEM.

environmental static cue (context) or auditory cue (tone) with an aversive unconditioned stimulus, usually an electrical footshock. After training, mice exposed to the same cues without the unconditioned stimulus elicit a natural defensive fear-induced freezing response, reflecting associative memory strength. During training, SIRT1-KO mice exhibited slightly higher activity levels than WT animals but showed similar exploratory movements, behavior, and footshock responses, including jumping, rushing, and freezing (Fig. 3 A). Short-term and long-term contextual associative memories were examined in the same training box without delivering the unconditioned stimulus 1.5 and 24 h after training, respectively. In both cases, SIRT1-KO mice showed significantly lower freezing behavior compared with WT mice (Fig. 3 B, C). To assess the ability of WT mice to discriminate the testing context, animals were transferred to a different box with a novel environment and static cues. Here, no difference between strains was observed in freezing responses (Fig. 3 D). Furthermore, WT mice showed the expected decrease in freezing behavior in response to a new context compared with that observed in the training box. In contrast, SIRT1-KO mice displayed similar freezing in the two contexts, confirming their impairment in associating the unconditioned stimulus with the training context (Fig. 3, compare C, D for each genotype). Next, we explored the ability of mice to associate an auditory cue to the unconditioned stimulus. In the altered context box, the same tone that preceded the electric

shock in the training phase was delivered and freezing behavior was monitored. SIRT1-KO mice exhibited a significantly lower freezing to tone compared with WT mice (Fig. 2E). Accordingly, gender analysis showed that both male and female animals lacking SIRT1 performed poorly in context-dependent tasks (supplemental Fig. S1D, available at www.jneurosci.org as supplemental material) and in fear conditioning to tone (supplemental Fig. S1E, available at www.jneurosci.org as supplemental material).

SIRT1 is necessary for normal spatial learning

We next explored spatial learning in SIRT1-KO mice using the Barnes maze. In this paradigm, mice were trained to locate the unique hole that leads to a black shelter box among 20 holes located around the perimeter of an open circular dry-land platform. To find the escape hole, mice must learn, memorize, and use the relationships among the visual cues in the room. Although both strains steadily improved in the ability to locate the target hole over the acquisition phase, SIRT1-KO mice exhibited a significantly lower percentage of success than WT mice (Fig. 4A). Accordingly, latency to locate the escape box decreased markedly faster in WT than in KO mice (Fig. 4B). This was accompanied by a reduced error rate in WT mice, which reached statistical significance at the end of the testing phase (Fig. 4C). When we analyzed the deviation between the first error and the target hole, we found that WT mice decreased deviation after day 4, whereas SIRT1-KO mice did not improve (Fig. 4D). Consistent with this, search strategy analysis indicated that SIRT1-KO mice used inferior strategies compared with WT mice. Although both strains initially used a random search (42% for WT vs 60% for KO), differences emerged over the course of the acquisition phase. WT mice rapidly abandoned the random strategy and steadily shifted to an equal use of spatial and serial strategies, and, by the end, spatial strategy represented 83% of their search pattern (Fig. 4E). In contrast, although SIRT1-KO animals decreased the use of the random strategy by half over the course of 6 d (from 60 to 30%), they only displayed a very limited use of direct search (20%) and eventually showed preference for the serial strategy (50%) (Fig. 4F). In addition, we found that, 7 d after the last training session, each genotype maintained its ability to solve the maze at a level similar to that on the last day of the acquisition phase (Fig. 4A–F, day 7 vs day 14), suggesting that memory retention is not affected in SIRT1-KO mice.

SIRT1 knock-out mice exhibit impaired long-term potentiation

The impairment in immediate, associative, and spatial memories but without visible neuroanatomical alterations in mice lacking
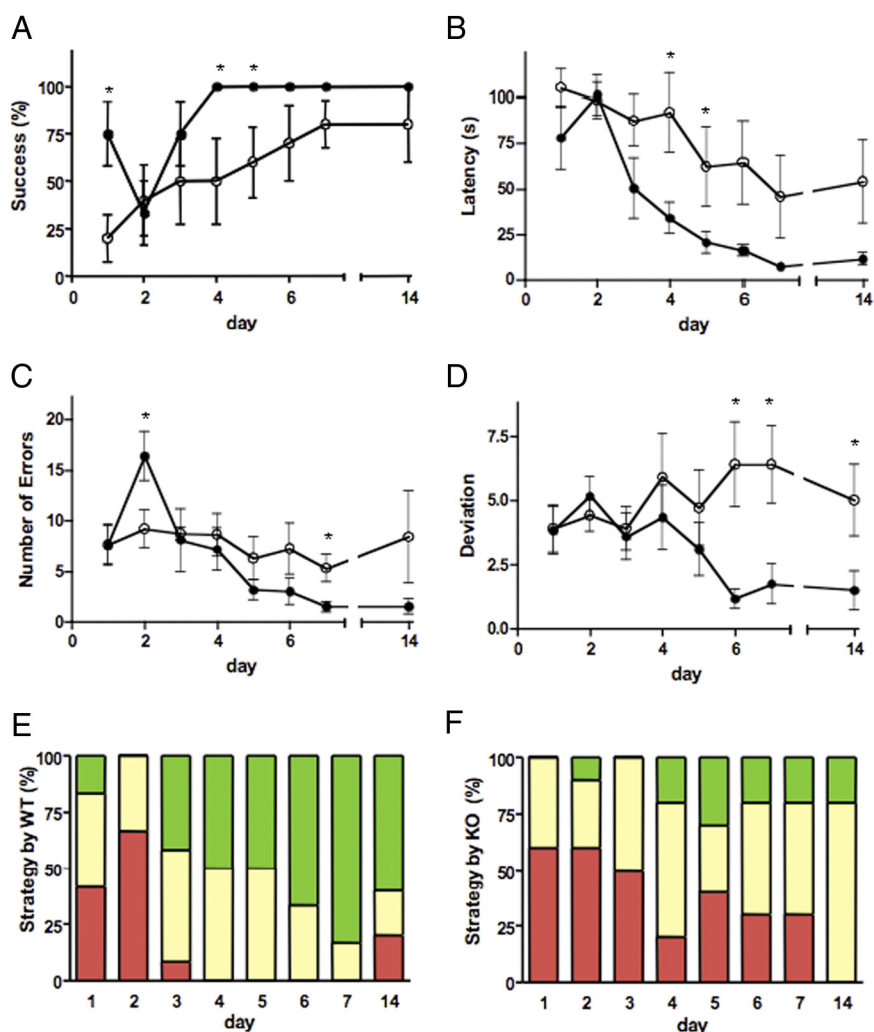

Figure 4. SIRT1-KO mice show spatial learning and memory impairment. **A**, Success of SIRT1-KO mice (*n* = 5; open circles) to find the escape box in the Barnes maze was lower than for WT mice (*n* = 6; *p* < 0.001; filled circles). **B**, Latency to find the escape box significantly decreased in WT mice compared with SIRT1-KO (*p* < 0.001). **C, D**, Number of total errors (**C**) and deviations from the first error (**D**) (*p* < 0.001) were both higher in SIRT1-KO mice than WT mice. **E, F**, Search strategy of WT (**E**) and SIRT1-KO (**F**) mice (serial strategy, yellow; spatial strategy, green; random strategy, red). Data represent means ± SEM. Statistical significance values correspond to the differences between curves analyzed all over the acquisition phase. *p* < 0.05, days with statistical significance.

SIRT1 led us to further investigate whether these learning deficits were correlated with defects in electrophysiological events underlying cognition such as LTP. To address this question, we first measured I/O responses produced by stimulation at different intensities of the Schaffer collateral pathway in hippocampus. As shown in Figure 5A, there was no significant difference in input/output curves between genotypes. Also, normal PPF was recorded in slices from SIRT1-KO mice (Fig. 5B), indicating that lack of SIRT1 does not cause a deleterious effect on basal synaptic transmission or presynaptic events at Schaffer collateral CA1 synapses.

We next assessed changes in long-lasting forms of synaptic plasticity by using two LTP protocols (Fig. 6A,B). Average fEPSP slopes measured 30–40 min after 5 × 3 theta burst stimulation (TBS) were not different between strains. However, hippocampal slices from SIRT1-KO mice exhibited significantly diminished LTP elicited by 10 × 10 TBS compared with WT (Fig. 5C,E), although short-term potentiation (STP) was normal (Fig. 5C,D). Because currents through NMDA receptor channels significantly
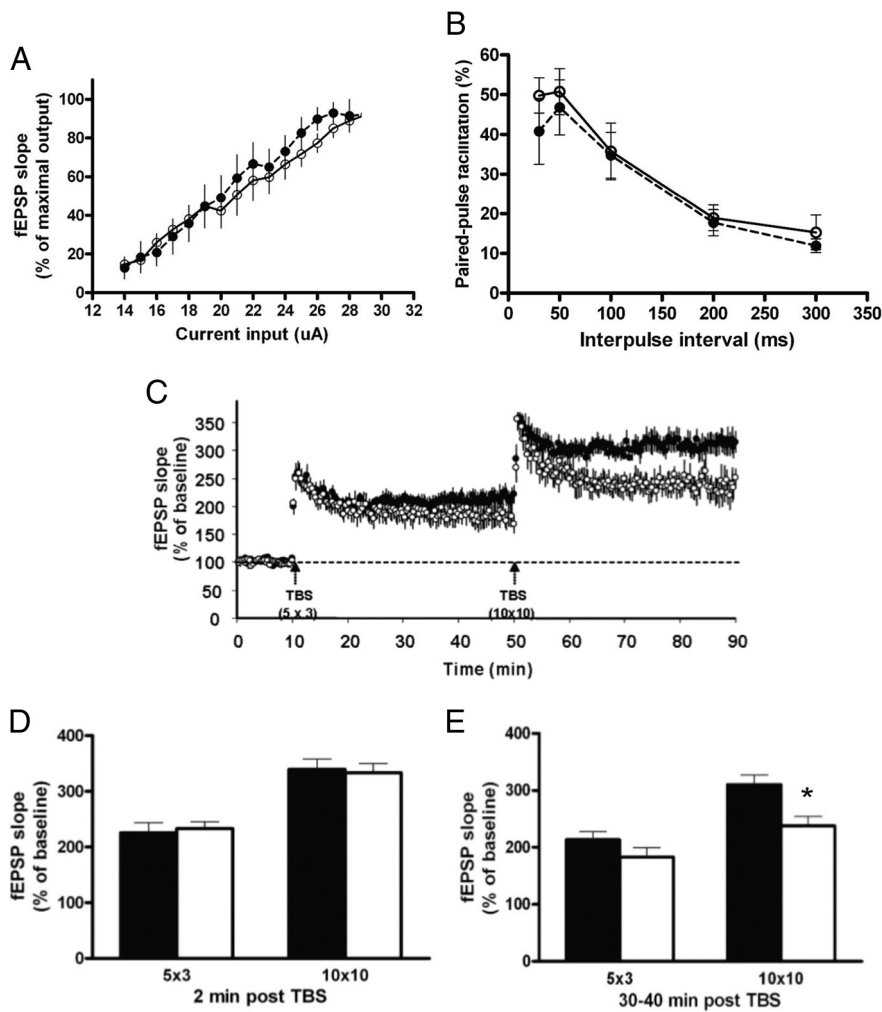
Figure 5. Lack of SIRT1 decreases hippocampal synaptic plasticity. *A*, I/O plots of field EPSP slopes versus current input (micro-amperes) were similar in WT (*n* = 7; filled circles) and SIRT1-KO (*n* = 8; open circles) mice, indicating that lack of SIRT1 does not alter baseline synaptic transmission. *B*, Paired-pulse facilitation (*n* = 3 each genotype) shows similar presynaptic plasticity in WT and SIRT1-KO mice. *C*, LTP in hippocampal CA1 field elicited by 5 × 3 and 10 × 10 TBS (EPSP slopes; WT, *n* = 5, filled circles; SIRT1-KO mice, *n* = 7, open circles). Five burst of 3 × 100 Hz stimulation evokes LTP in both genotypes, whereas 10 bursts of 10 × 100 Hz trains stimulation leads to a long-lasting form of LTP in control but not in SIRTI-KO mouse. *D*, EPSP slopes averages during the first 2 min after TBS (short-term potentiation) were similar in both genotypes. *E*, EPSP slopes averages 30–40 min after applying the 10 × 10 TBS protocol show significant differences in LTP induction in WT animals compared with SIRT1-KO mice (*$p < 0.05$, *t* test). Data represent means ± SEM.

performed a morphometric analysis of dendritic spines in CA1 pyramidal neurons stained by Golgi staining. Spine density on CA1 apical trees in stratum radiatum was similar in WT and SIRT1-KO mice when analyzed per segment, neuron, or brain. Different subtypes of spines, including filopodia, dimple, nubby, mushroom, and lollipop, were found in similar numbers in both phenotypes (supplemental Table S1, available at www.jneurosci.org as supplemental material). In contrast, we found significant differences in dendritic arborization of granule cells in the dentate gyrus between WT and SIRT1-KO mice, whereas spine density or soma size were conserved (data not shown). As revealed by the Sholl analysis, SIRT1-KO mice showed significantly less dendritic material at all distances from neuronal soma (Fig. 7*A*). The cumulative total number of intersections with the Sholl concentric circles (e.g., total hits), which estimates total dendritic length, indicated that dendritic arbors in SIRT1-KO mice have significantly less dendritic length than in WT mice (Fig. 7*B*). Accordingly, determination of the number of bifurcation branch points in the dendritic arbor demonstrated that neurons from SIRT1-KO mice have significantly less dendritic complexity compared with WT mice (Fig. 7*C*). Although not significant, the complexity ratio, determined by the number of terminal tip segments over the number of primary branches emanating from the soma, exhibited a similar decrease in SIRT1-KO mice. Together, our data suggest that lack of SIRT1 was not associated with abnormalities in spine architecture but rather with marked alterations in the conformation of neuronal dendritic trees.

participate in the overall burst responses, we determined whether NMDA receptor function was altered in SIRT1-KO hippocampus. Analysis of synaptic responses during theta bursts did not reveal significant differences between slices from SIRT1-KO and WT mice, suggesting that LTP deficits in SIRT1-KO mice were not attributable to alterations in NMDA receptor function (Fig. 6*C,D*). Together, these results indicate that the lack of SIRT1 in hippocampal neurons does not modify the basic features of synaptic transmission but results in a substantial deficit in LTP at CA3–CA1 synapses.

Conserved dendritic spine structure but altered dendritic architecture in neurons of SIRT1-KO mice
CA1 pyramidal cells and their dendritic spines play a major role in the trisynaptic circuit, thus importantly impacting memory acquisition and LTP. Number, size, and shape of dendritic spines are critical parameters for determining neuronal function and provide the structural bases of synaptic plasticity. Therefore, we

Altered gene expression in hippocampus of SIRT1-KO mice
We next analyzed whether spatial or associative learning modified SIRT1 levels in hippocampus. Western blots of wild-type mice trained in the fear conditioning (contextual/tone) and water maze (supplemental Fig. S3*C–E*, available at www.jneurosci.org as supplemental material) showed that SIRT1 levels were not changed at 1 or 24 h after fear conditioning (supplemental Fig. S3*A*, available at www.jneurosci.org as supplemental material) and at 14 d of water maze training (supplemental Fig. S3*B*, available at www.jneurosci.org as supplemental material). We also assessed whether levels of SIRT1 in hippocampus may be regulating the levels of proteins involved in synaptic signaling in hippocampal neurons. Protein extracts of isolated hippocampi analyzed by Western blots had similar levels of synapsin and synaptophysin (supplemental Fig. S2*A*, available at www.jneurosci.org as supplemental material). However, as we showed previously, ERK1/2 phosphorylation was decreased in hippocampus of SIRT1-KO mice (data not shown) (Li et al., 2008).

Regulation of gene expression also plays a key role in memory, learning, and synaptic plasticity. Because we showed previously that SIRT1 regulates important transcriptional changes during aging in mouse cerebral cortex, we examined SIRT1-dependent gene regulation in hippocampus. RNA harvested from WT and SIRT1-KO was analyzed using Affymetrix gene chips. We found that only few transcripts in SIRT1-KO were detected at levels that differed by 1.3-fold from WT (supplemental Fig. S2 B, Table S2, available at www.jneurosci.org as supplemental material). Among the genes differentially regulated in SIRT1- KO hippocampi were those involved in synaptic function, membrane fusion, myelination, and amino acid and lipid metabolism (supplemental Fig. S2 C, available at www.jneurosci.org as supplemental material). Interestingly, some of those genes are also regulated by IGF-1, IRS-2, and/or ERK1/2, as shown in supplemental Table S3 (available at www.jneurosci.org as supplemental material).

High levels of SIRT1 in hippocampus has no effect on synaptic plasticity or memory

Next, we tested whether higher SIRT1 levels in hippocampal neurons would be sufficient to enhance LTP. To increase brain SIRT1 levels, we bred the floxed SIRT1 transgenic mice (Firestein et al., 2008) with the brain-specific Nestin–Cre mice (Tronche et al., 1999). Hippocampus of double-transgenic mice (referred to as NeSTO) expressed 16-fold excess of SIRT1 compared with levels in Nestin–Cre control mice, as assessed by Western blots (Fig. 8 A). Brain immunohistochemistry indicated that SIRT1 in transgenic NeSTO mice was distributed like the endogenous protein in granule cells of the dentate gyrus as well as in pyramidal neurons of CA1 and CA3. In addition, overexpressed SIRT1 also colocalized with NeuN and DAPI but not with the glial protein GFAP (supplemental Fig. S4, available at www.jneurosci.org as supplemental material).

Electrophysiological data obtained in hippocampal slices from NeSTO and Nestin–Cre mice showed that the I/O curve was shifted to the left in NeSTO mice compared with that in Nestin–Cre mice (Fig. 8 B), suggesting increased basal synaptic excitability. However, no significant differences between genotypes were detected in PPF (Fig. 8 C), STP or LTP (Fig. 8 D), or 5 × 3 TBS burst responses (Fig. 6 E). In contrast to the SIRT1-KO results, NeSTO hippocampal neurons exhibited a significant facilitation in 10 × 10 TBS burst responses (Fig. 6 F). Thus, SIRT1 overexpression in the hippocampus does not alter synaptic plasticity, although it results in increased excitability, possibly as a result of changes in some properties of AMPA receptors.
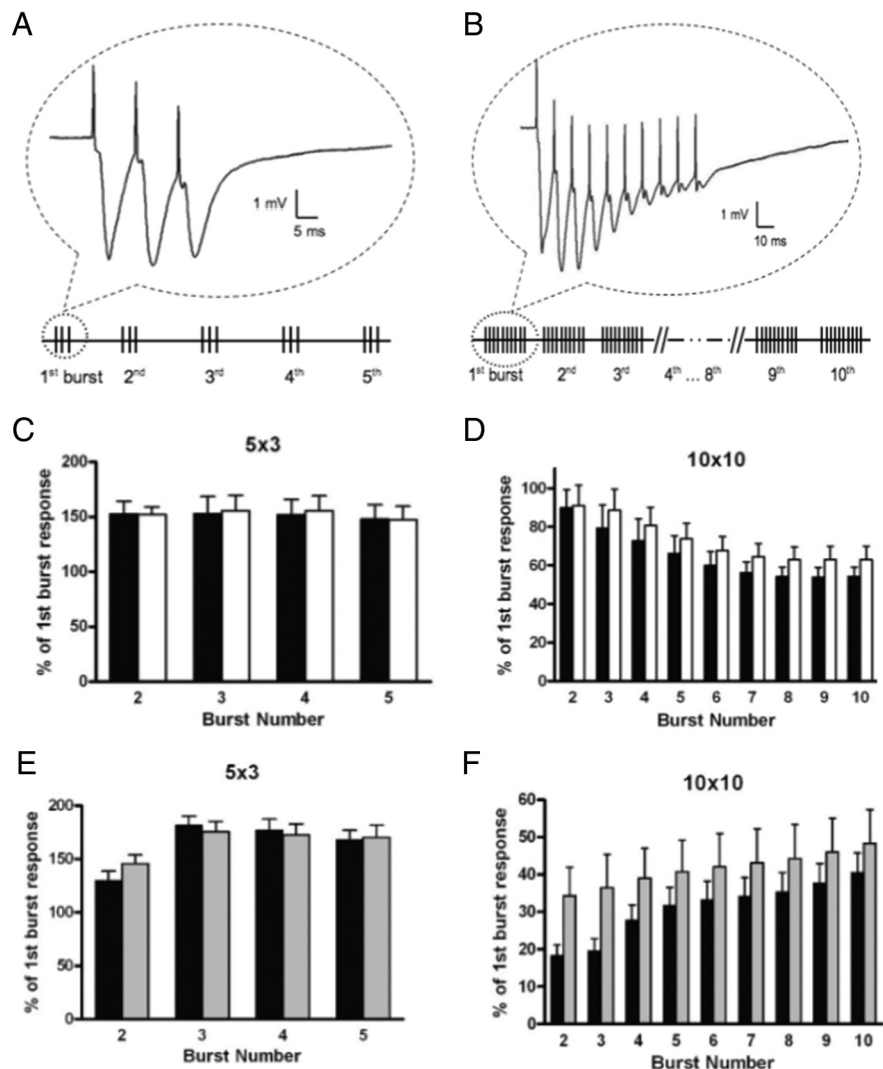

Figure 6. Burst responses in field CA1 of hippocampal slices from SIRT1-KO and NeSTO mice. Two different protocols of TBS, followed by 40 min of test-pulse recording were used. **A**, 5 × 3 TBS, five bursts at 5 Hz (theta burst), each burst consisting of three pulses at 100 Hz. **B**, 10 × 10 TBS, 10 theta bursts, each burst consisting of 10 pulses at 100 Hz. The duration of each pulse within TBS was double that of the test pulse. For each burst response during LTP induction, the area under the curve was measured and each burst area was normalized to the first burst area. (The bottom panels of simulated responses were not scaled.) **C, D**, SIRT1-KO (open circles) and WT (filled circles) burst responses elicited by 5 × 3 TBS (**C**) and 10 × 10 TBS (**D**). **E, F**, NeSTO (gray bars) and Nestin–Cre (black bars) burst responses elicited by 5 × 3 TBS (**E**) and 10 × 10 TBS (**F**) ($p < 0.005$, two-way ANOVA). Data represent mean ± SEM.

We also tested whether increased SIRT1 levels in hippocampus could elicit behavioral effects opposite to those observed in knock-out mice, for instance, by promoting improved associative learning. In agreement with the LTP results, we did not detect any differences in fear conditioning to either context (Fig. 8 E) or tone (Fig. 8 F) between NeSTO and Nestin–Cre mice, even when two different mice cohorts were trained with two different protocols, receiving five (Fig. 8 E) or three (supplemental Fig. S5 B,C, available at www.jneurosci.org as supplemental material) footshocks during training. We also tested spatial memory in the water maze (supplemental Fig. S5 D,E, available at www.jneurosci.org as supplemental material) and object recognition memory (Fig. S5 A) and again did not find any differences (data not shown). Together, the data obtained with the transgenic mice suggest that high levels of SIRT1 in brain neither impair nor enhance cognition.
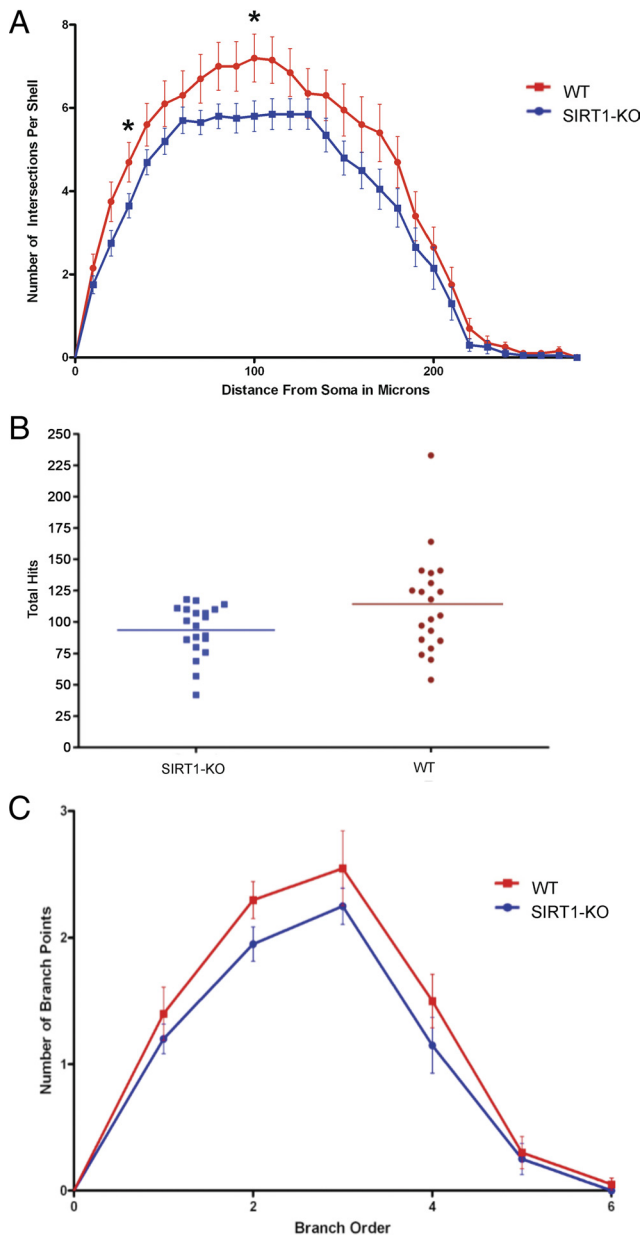
Figure 7. Neuronal dendritic trees from SIRT1-KO mice show less branching and complexity than WT mice. **A**, Sholl analysis shows significantly less dendritic material over the entire neuronal tree in SIRT1-KO mice; $p < 0.0001$. **B**, Dendritic branch length was 22% lower in SIRT1-KO (100 ± 5.1%) than WT mice (122 ± 10%; $p < 0.05$). **C**, Neuronal dendritic arbors show less complexity in SIRT-KO mice ($p < 0.05$). SIRT1-KO and WT for all analysis correspond to $n = 4$ brain and $n = 20$ neurons (5 neurons per brain). Data represent mean ± SEM. Statistical significance values correspond to the differences between curves analyzed over the entire neuronal trees. Asterisks show the shells from the soma with statistical significance of $p < 0.05$.

Discussion

Our results indicate that SIRT1 plays an important role in cellular mechanisms underlying learning and memory in mice. Here we show that SIRT1 localizes in the nuclei of pyramidal and granule neurons of the hippocampus, a structure critically involved in cognitive processes. The lack of SIRT1 leads to significant behavioral alterations in different classical paradigms assessing formation of immediate, associative, and spatial memo-

ries. Although SIRT1-KO mice exhibit normal exploratory behavior in the open field and discriminatory ability in the novel object recognition test, a significant deficit in immediate memory was revealed by decreased spontaneous alternation in the Y maze. However, hippocampal-dependent memories showed the most dramatic impairment. The negligible fear behavior exhibited by SIRT1-KO mice when assessed for contextual associative memory compared with the ability of WT mice to discriminate between training and novel contexts tested at either short term or long term, together with the impaired spatial abilities of mutant animals in the Barnes maze, indicate the important role of SIRT1 in hippocampus-dependent cognitive learning. Although SIRT1-KO mice are less spontaneously active than WT mice (Boily et al., 2008), we found that activity levels displayed during each cognitive test were similar or even higher in SIRT1-KO mice compared with WT mice perhaps because these tests performed during the inactive (light) period. In addition, despite the delayed and incomplete eyelid opening in knock-out animals (McBurney et al., 2003), our tests of pupillary reflexes, visual perception, and cues, together with the normal capacity of object identification and discrimination in the NORT, indicated that their visual functions were unaltered. In accordance, eye size, lens, and retina appeared to be normal in both WT and SIRT1 knock-out mice. Thus, our data suggest that neither the lethargic phenotype nor the eyelid defect is likely to account for the impaired behavioral performance in SIRT1-KO mice.

In agreement with our behavioral results, LTP, which is widely considered to represent a cellular mechanism for the formation of specific types of memory, including spatial and contextual learning (McHugh et al., 1996; Chen and Tonegawa, 1997), was impaired in SIRT1-KO mice. In contrast, STP as well as basic electrophysiological properties of synaptic transmission, including presynaptic mechanisms and ionotropic receptor functions, were unaltered in SIRT1-deficient mice, suggesting that SIRT1 acts downstream of glutamate receptors to regulate LTP formation/consolidation. Based on our data, SIRT1 deletion does not impair LTP induction but instead impairs the maximum expression of LTP. One possibility is that SIRT1 participates in the regulation of AMPA receptor trafficking.

Despite the fact that SIRT1-KO mice have reduced body and organ sizes, including brain size, which is 20% smaller than that of WT mice (Boily et al., 2008), we did not find alterations in gross brain architecture. In addition, normal dendritic spine density and morphology of CA1 pyramidal neurons, as well as normal expression of synapsin and synaptophysin in SIRT1-KO mice, suggest that neither microanatomical differences in spine structure or alterations in levels of synaptic proteins could account for the synaptic plasticity deficits found in SIRT1-KO mice. However, the significant decreases in branching, length, and complexity of neuronal dendritic arborizations of granule cells in the dentate gyrus of SIRT1-KO mice could explain some of the phenotypic differences with WT animals. Furthermore, the decreased dendritic complexity observed in SIRT1-KO mice may be related to their small brain size, similarly to other genes disruptions such as IGF-1 (Beck et al., 1995; Niblock et al., 2000), BDNF (Patterson et al., 1996; Gorski et al., 2003), or methyl-CpG binding protein 2 (Zhou et al., 2006), in which brain size closely correlates with dendritic conformation.

It is well documented that changes in the levels of histone acetylation modify synaptic plasticity and learning abilities

(Alarcón et al., 2004; Levenson et al., 2004a; Fischer et al., 2007). Regulation of chromatin remodeling and gene expression through histone acetylation is critical in memory consolidation (Levenson et al., 2004b). Specific inhibitors of Class I, II, and IV HDACs, such as TSA and sodium butyrate, have been shown to induce dendritic sprouting, increase the number of synapses, and reverse LTP and memory deficits observed under various conditions (Alarcón et al., 2004; Fischer et al., 2007). In contrast, our data show that a lack of SIRT1, an NAD$^+$-dependent HDAC (Class III), leads to memory and synaptic plasticity impairment, indicating that both types of histone deacetylases play essential roles in cognition, although their activities differentially impact molecular and cellular process underlying learning and memory. These results indicate that more information is required regarding the identity and functions of the targets of these different classes of deacetylases.

Although the gene expression differences in the microarray between SIRT1-KO and WT hippocampus were small, we identified deregulation in the expression of genes involved in synaptic function, membrane fusion, myelination, and lipid and amino acid metabolism. However, to link these changes in gene expression with the memory impairments observed in SIRT1-KO mice, it is necessary to test the role of reduced expression of a number of these genes in the behavior phenotypes of the SIRT1-KO mice.

The regulation of insulin/IGF-1 signaling and IRS-2/ERK1/2 pathway may also contribute to the effect of SIRT1 in mouse cognition. SIRT1 upregulates IGF-1 by either derepressing IGF binding protein-1 (Lemieux et al., 2005) or deacetylating IRS-2 (Zhang, 2007; Li et al., 2008). In turn, reduction of IGF-1 signaling can decrease the downstream mitogen-activated protein kinase (MAPK), ERK1/2, and phosphatidylinositol 3 kinase, which are important for various brain functions (Zhang, 2007; Huang et al., 2008). Mice with reduced IGF-1 levels have impaired spatial learning, and this effect is partially reversed by IGF-1 replenishment (Trejo et al., 2007). In agreement with this, brain-specific SIRT1 mutant mice show somatotropic axis disruption and a marked IGF-1 reduction (Cohen et al., 2009). Also, MAPK activation is required for several forms of LTP and for spatial learning and fear conditioning (Selcher et al., 1999). In addition, activation of ERK1/2 has been shown to be associated with LTP induction as well as with learning and memory (Trifilieff et al., 2007). We showed previously that SIRT1 inhibition reduces ERK1/2 activity in part through the inactivation of IRS-2 and that ERK1/2 phosphorylation decreases in hippocampus of SIRT1-KO mice (Li et al., 2008). Interestingly,
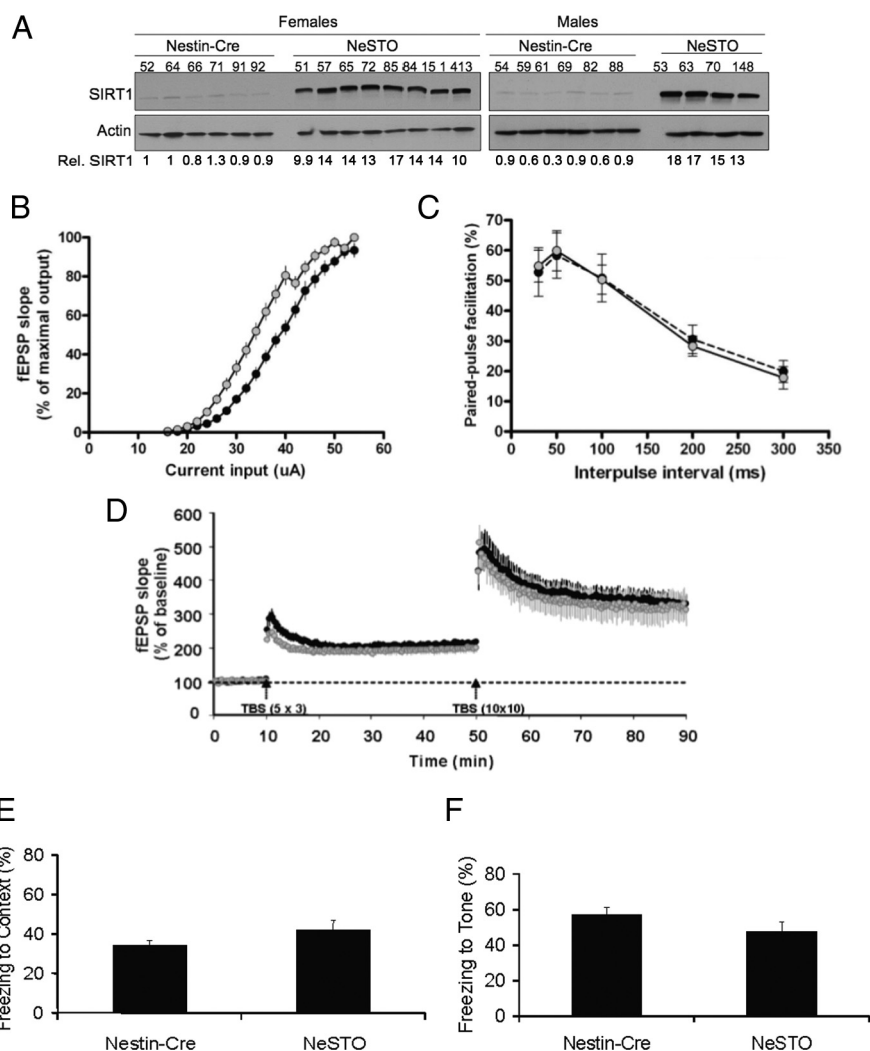

Figure 8. Overexpression of SIRT1 in hippocampus does not alter LTP or associative memory. **A**, Western blot shows ∼16-fold SIRT1 protein increase in hippocampus of NeSTO mice compared with control Nestin−Cre animals. The numbers below show SIRT1 levels relative to actin. **B**, I/O curve of field EPSP slope versus current input (microamperes) is shifted to the left in NeSTO mice ($n = 14$; gray circles) compared with Nestin−Cre ($n = 10$; black circles; $p < 0.0001$, two-way ANOVA), suggesting increased basal synaptic excitability. **C**, Paired-pulse facilitation reveals normal presynaptic events in NeSTO mice ($n = 5$ each genotype). **D**, Similar LTP was elicited by 5 × 3 and 10 × 10 TBS (EPSP slopes; $n = 7$ each genotype) in mice overexpressing wild-type or increased levels of SIRT1. **E**, **F**, Fear conditioning to context (**E**) or tone (**F**) in Nestin−Cre ($n = 14$) and NeSTO animals ($n = 18$) show similar associative learning capacities in both strains. Data represent means ± SEM.

we found that several genes regulated by SIRT1 in hippocampus involved in myelination or lipid metabolism are also regulated by IGF-1, IRS-2, and/or ERK1/2 (supplemental Table S3, available at www.jneurosci.org as supplemental material). Thus, SIRT1 may function as a coordinator of multiple proteins/enzymes involved in IGF-1 signaling, ranging from IGF-1 binding proteins, to key components of the IGF-IR signaling pathway involved in learning and memory, such as MAPK and ERK1/2.

In contrast to the SIRT1-KO mice, increased brain levels of SIRT1 in NeSTO mice did not affect LTP, immediate, spatial, or associative memory, although these mice exhibited increased synaptic excitability, possibly as a result of changes in some properties of AMPA receptors. Normal synaptic plasticity, together with unaltered associative learning in NeSTO

mice, led us to propose that the high levels of SIRT1 protein (~16-fold increase than WT) reached in the hippocampus of the transgenic mice may interfere with the potential effects of SIRT1 overexpression. Thus, it is possible that LTP and cognitive abilities might become unresponsive to the excessive amounts of SIRT1 in NeSTO mouse brain. In agreement with this idea, previous studies have shown that only low to moderate levels of SIRT1 overexpression confer beneficial effects in mouse heart (up to 7.5-fold) (Alcendor et al., 2007), intestine (Firestein et al., 2008), and bone marrow lymphocyte progenitors (Oberdoerffer et al., 2008) (threefold to fourfold in both cases). Alternatively, it is possible that the excess protein did not assemble into the appropriate protein complexes or that an NAD^+ decrease may have compensated for increased SIRT1 levels. Also, it is important to stress that our NeSTO animals, which showed no alterations in LTP and memory, were analyzed at a relatively young age; it is therefore possible that the effects of SIRT1 overexpression in cognition would become evident during the course of aging. Interestingly, a recent study shows that old but not young mice overexpressing SIRT1 exhibited differences in NORT tested 24 h after training (Kakefuda et al., 2009). Performing learning tests in older NeSTO animals together with ongoing studies using SIRT1 agonists in transgenic mice should provide more insights regarding the effect of SIRT1 overexpression on cognition.

Memory and synaptic plasticity are highly vulnerable to decline with aging. Calorie restriction (CR) is a dietary regimen that attenuates age-dependent degenerative processes, as well as both cognitive deficits and synaptic plasticity (Weindruch et al., 1986; Roth et al., 1995; Fontán-Lozano et al., 2007; Pearson et al., 2008). SIRT1 is a potential mediator of the beneficial effects conferred by CR (Cohen et al., 2004; Guarente, 2005), and it was shown recently that CR does not increase lifespan of SIRT1-KO mice (Boily et al., 2008; Li et al., 2008). Thus, our findings raise the question of the potential role of this protein in CR-mediated improvement of cognitive performance. However, here we found that the deficit in synaptic plasticity caused by the lack of SIRT1 is independent of NMDA receptors, opposite to the NMDA receptor-dependent synaptic plasticity facilitation by CR (Fontán-Lozano et al., 2007), and that high levels of SIRT1 in brain do not alter synaptic plasticity.

In summary, our results indicate that the NAD^+-dependent deacetylase SIRT1 is critical for maintaining normal acquisition and consolidation of short-term and long-term hippocampus-dependent memories and synaptic plasticity, without modifying basal synaptic properties, dendritic spine structure of CA1 neurons, or synaptic proteins levels. An important decrease in neuronal dendritic tree arborization, branch length, and complexity may account for some of the deficits observed in SIRT1-KO mice. Also, our work suggests that deficiency in the ERK1/2/MAPK pathway in combination with altered expression of genes involved in synaptic functions and myelination are some of the mechanisms through which SIRT1 may regulate memory, learning, and synaptic plasticity in hippocampus. Additional studies should provide insights into the unknown molecular mechanisms through which SIRT1 regulates normal mouse cognitive function.

References

Ahn HJ, Hernandez CM, Levenson JM, Lubin FD, Liou HC, Sweatt JD (2008) c-Rel, an NF-kappaB family transcription factor, is required for hippocampal long-term synaptic plasticity and memory formation. Learn Mem 15:539–549.

Alarcón JM, Malleret G, Touzani K, Vronskaya S, Ishii S, Kandel ER, Barco A (2004) Chromatin acetylation, memory, and LTP are impaired in CBP+/− mice: a model for the cognitive deficit in Rubinstein-Taybi syndrome and its amelioration. Neuron 42:947–959.

Alcendor RR, Gao S, Zhai P, Zablocki D, Holle E, Yu X, Tian B, Wagner T, Vatner SF, Sadoshima J (2007) Sirt1 regulates aging and resistance to oxidative stress in the heart. Circ Res 100:1512–1521.

Asher G, Gatfield D, Stratmann M, Reinke H, Dibner C, Kreppel F, Mostoslavsky R, Alt FW, Schibler U (2008) SIRT1 regulates circadian clock gene expression through PER2 deacetylation. Cell 134:317–328.

Bach ME, Hawkins RD, Osman M, Kandel ER, Mayford M (1995) Impairment of spatial but not contextual memory in CaMKII mutant mice with a selective loss of hippocampal LTP in the range of the theta frequency. Cell 81:905–915.

Barbosa AC, Kim MS, Ertunc M, Adachi M, Nelson ED, McAnally J, Richardson JA, Kavalali ET, Monteggia LM, Bassel-Duby R, Olson EN (2008) MEF2C, a transcription factor that facilitates learning and memory by negative regulation of synapse numbers and function. Proc Natl Acad Sci U S A 105:9391–9396.

Barnes CA (1979) Memory deficits associated with senescence: a neurophysiological and behavioral study in the rat. J Comp Physiol Psychol 93:74–104.

Beck KD, Powell-Braxton L, Widmer HR, Valverde J, Hefti F (1995) Igf1 gene disruption results in reduced brain size, CNS hypomyelination, and loss of hippocampal granule and striatal parvalbumin-containing neurons. Neuron 14:717–730.

Boily G, Seifert EL, Bevilacqua L, He XH, Sabourin G, Estey C, Moffat C, Crawford S, Saliba S, Jardine K, Xuan J, Evans M, Harper ME, McBurney MW (2008) SirT1 regulates energy metabolism and response to caloric restriction in mice. PLoS ONE 3:e1759.

Chen C, Tonegawa S (1997) Molecular genetic analysis of synaptic plasticity, activity-dependent neural development, learning, and memory in the mammalian brain. Annu Rev Neurosci 20:157–184.

Chen J, Zhou Y, Mueller-Steiner S, Chen LF, Kwon H, Yi S, Mucke L, Gan L (2005) SIRT1 protects against microglia-dependent amyloid-beta toxicity through inhibiting NF-kappaB signaling. J Biol Chem 280:40364–40374.

Cheng HL, Mostoslavsky R, Saito S, Manis JP, Gu Y, Patel P, Bronson R, Appella E, Alt FW, Chua KF (2003) Developmental defects and p53 hyperacetylation in Sir2 homolog (SIRT1)-deficient mice. Proc Natl Acad Sci U S A 100:10794–10799.

Cohen DE, Supinski AM, Bonkowski MS, Donmez G, Guarente LP (2009) Neuronal SIRT1 regulates endocrine and behavioral responses to calorie restriction. Gene Dev 23:2812–2817.

Cohen HY, Miller C, Bitterman KJ, Wall NR, Hekking B, Kessler B, Howitz KT, Gorospe M, de Cabo R, Sinclair DA (2004) Calorie restriction promotes mammalian cell survival by inducing the SIRT1 deacetylase. Science 305:390–392.

Ennaceur A, Neave N, Aggleton JP (1997) Spontaneous object recognition and object location memory in rats: the effects of lesions in the cingulate cortices, the medial prefrontal cortex, the cingulum bundle and the fornix. Exp Brain Res 113:509–519.

Firestein R, Blander G, Michan S, Oberdoerffer P, Ogino S, Campbell J, Bhimavarapu A, Luikenhuis S, de Cabo R, Fuchs C, Hahn WC, Guarente LP, Sinclair DA (2008) The SIRT1 deacetylase suppresses intestinal tumorigenesis and colon cancer growth. PLoS ONE 3:e2020.

Fischer A, Sananbenesi F, Wang X, Dobbin M, Tsai LH (2007) Recovery of learning and memory is associated with chromatin remodelling. Nature 447:178–182.

Fontán-Lozano A, Sáez-Cassanelli JL, Inda MC, de los Santos-Arteaga M, Sierra-Domínguez SA, López-Lluch G, Delgado-García JM, Carrión AM (2007) Caloric restriction increases learning consolidation and facilitates synaptic plasticity through mechanisms dependent on NR2B Subunits of the NMDA receptor. J Neurosci 27:10185–10195.

Fulco M, Cen Y, Zhao P, Hoffman EP, McBurney MW, Sauve AA, Sartorelli V (2008) Glucose restriction inhibits skeletal myoblast differentiation by activating SIRT1 through AMPK-mediated regulation of Nampt. Dev Cell 14:661–673.

Gautier L, Cope L, Bolstad BM, Irizarry RA (2004) affy–analysis of Af-

fymetrix GeneChip data at the probe level. Bioinformatics 20:307–315.

Gorski JA, Zeiler SR, Tamowski S, Jones KR (2003) Brain-derived neurotrophic factor is required for the maintenance of cortical dendrites. J Neurosci 23:6856–6865.

Guarente L (2005) Calorie restriction and SIR2 genes: towards a mechanism. Mech Ageing Dev 126:923–928.

Hasegawa K, Yoshikawa K (2008) Necdin regulates p53 acetylation via Sirtuin1 to modulate DNA damage response in cortical neurons. J Neurosci 28:8772–8784.

Hisahara S, Chiba S, Matsumoto H, Tanno M, Yagi H, Shimohama S, Sato M, Horio Y (2008) Histone deacetylase SIRT1 modulates neuronal differentiation by its nuclear translocation. Proc Natl Acad Sci U S A 105:15599–15604.

Huang J, Gan Q, Han L, Li J, Zhang H, Sun Y, Zhang Z, Tong T (2008) SIRT1 overexpression antagonizes cellular senescence with activated ERK/S6k1 signaling in human diploid fibroblasts. PLoS ONE 3:e1710.

Hughes RN (2004) The value of spontaneous alternation behavior (SAB) as a test of retention in pharmacological investigations of memory. Neurosci Biobehav Rev 28:497–505.

Kaeberlein M, McVey M, Guarente L (1999) The SIR2/3/4 complex and SIR2 alone promote longevity in Saccharomyces cerevisiae by two different mechanisms. Gene Dev 13:2570–2580.

Kakefuda K, Fujita Y, Oyagi A, Hyakkoku K, Kojima T, Umemura K, Tsuruma K, Shimazawa M, Ito M, Nozawa Y, Hara H (2009) Sirtuin 1 overexpression mice show a reference memory deficit, but not neuroprotection. Biochem Biophys Res Commun 387:784–788.

Kim D, Nguyen MD, Dobbin MM, Fischer A, Sananbenesi F, Rodgers JT, Delalle I, Baur JA, Sui G, Armour SM, Puigserver P, Sinclair DA, Tsai LH (2007) SIRT1 deacetylase protects against neurodegeneration in models for Alzheimer's disease and amyotrophic lateral sclerosis. EMBO J 26:3169–3179.

Kim JE, Chen J, Lou Z (2008) DBC1 is a negative regulator of SIRT1. Nature 451:583–586.

Lee IH, Cao L, Mostoslavsky R, Lombard DB, Liu J, Bruns NE, Tsokos M, Alt FW, Finkel T (2008) A role for the NAD-dependent deacetylase Sirt1 in the regulation of autophagy. Proc Natl Acad Sci U S A 105:3374–3379.

Lemieux ME, Yang X, Jardine K, He X, Jacobsen KX, Staines WA, Harper ME, McBurney MW (2005) The Sirt1 deacetylase modulates the insulin-like growth factor signaling pathway in mammals. Mech Ageing Dev 126:1097–1105.

Levenson JM, O'Riordan KJ, Brown KD, Trinh MA, Molfese DL, Sweatt JD (2004a) Regulation of histone acetylation during memory formation in the hippocampus. J Biol Chem 279:40545–40559.

Levenson JM, Choi S, Lee SY, Cao YA, Ahn HJ, Worley KC, Pizzi M, Liou HC, Sweatt JD (2004b) A bioinformatics analysis of memory consolidation reveals involvement of the transcription factor c-Rel. J Neurosci 24:3933–3943.

Li C, Hung Wong W (2001) Model-based analysis of oligonucleotide arrays: model validation, design issues and standard error application. Genome Biol 2:RESEARCH0032.1–0032.11.

Li C, Wong WH (2001) Model-based analysis of oligonucleotide arrays: expression index computation and outlier detection. Proc Natl Acad Sci U S A 98:31–36.

Li X, Zhang S, Blander G, Tse JG, Krieger M, Guarente L (2007) SIRT1 deacetylates and positively regulates the nuclear receptor LXR. Mol Cell 28:91–106.

Li Y, Xu W, McBurney MW, Longo VD (2008) SirT1 inhibition reduces IGF-I/IRS-2/Ras/ERK1/2 signaling and protects neurons. Cell Metab 8:38–48.

Luo J, Nikolaev AY, Imai S, Chen D, Su F, Shiloh A, Guarente L, Gu W (2001) Negative control of p53 by Sir2alpha promotes cell survival under stress. Cell 107:137–148.

McBurney MW, Yang X, Jardine K, Hixon M, Boekelheide K, Webb JR, Lansdorp PM, Lemieux M (2003) The mammalian SIR2 alpha protein has a role in embryogenesis and gametogenesis. Mol Cell Biol 23:38–54.

McHugh TJ, Blum KI, Tsien JZ, Tonegawa S, Wilson MA (1996) Impaired hippocampal representation of space in CA1-specific NMDAR1 knockout mice. Cell 87:1339–1349.

Meffert MK, Chang JM, Wiltgen BJ, Fanselow MS, Baltimore D (2003) NF-kappa B functions in synaptic signaling and behavior. Nat Neurosci 6:1072–1078.

Michan S, Sinclair D (2007) Sirtuins in mammals: insights into their biological function. Biochem J 404:1–13.

Niblock MM, Brunso-Bechtold JK, Riddle DR (2000) Insulin-like growth factor I stimulates dendritic growth in primary somatosensory cortex. J Neurosci 20:4165–4176.

Oberdoerffer P, Michan S, McVay M, Mostoslavsky R, Vann J, Park SK, Hartlerode A, Stegmuller J, Hafner A, Loerch P, Wright SM, Mills KD, Bonni A, Yankner BA, Scully R, Prolla TA, Alt FW, Sinclair DA (2008) DNA damage-induced alterations in chromatin contribute to genomic integrity and age-related changes in gene expression. Cell 135:907–918.

Pallàs M, Pizarro JG, Gutierrez-Cuesta J, Crespo-Biel N, Alvira D, Tajes M, Yeste-Velasco M, Folch J, Canudas AM, Sureda FX, Ferrer I, Camins A (2008) Modulation of SIRT1 expression in different neurodegenerative models and human pathologies. Neuroscience 154:1388–1397.

Patterson SL, Abel T, Deuel TA, Martin KC, Rose JC, Kandel ER (1996) Recombinant BDNF rescues deficits in basal synaptic transmission and hippocampal LTP in BDNF knockout mice. Neuron 16:1137–1145.

Pearson KJ, Lewis KN, Price NL, Chang JW, Perez E, Cascajo MV, Tamashiro KL, Poosala S, Csiszar A, Ungvari Z, Kensler TW, Yamamoto M, Egan JM, Longo DL, Ingram DK, Navas P, de Cabo R (2008) Nrf2 mediates cancer protection but not prolongevity induced by caloric restriction. Proc Natl Acad Sci U S A 105:2325–2330.

Picard F, Kurtev M, Chung N, Topark-Ngarm A, Senawong T, Machado De Oliveira R, Leid M, McBurney MW, Guarente L (2004) Sirt1 promotes fat mobilization in white adipocytes by repressing PPAR-gamma. Nature 429:771–776.

Prozorovski T, Schulze-Topphoff U, Glumm R, Baumgart J, Schröter F, Ninnemann O, Siegert E, Bendix I, Brüstle O, Nitsch R, Zipp F, Aktas O (2008) Sirt1 contributes critically to the redox-dependent fate of neural progenitors. Nat Cell Biol 10:385–394.

Qin W, Yang T, Ho L, Zhao Z, Wang J, Chen L, Zhao W, Thiyagarajan M, MacGrogan D, Rodgers JT, Puigserver P, Sadoshima J, Deng H, Pedrini S, Gandy S, Sauve AA, Pasinetti GM (2006) Neuronal SIRT1 activation as a novel mechanism underlying the prevention of Alzheimer disease amyloid neuropathology by calorie restriction. J Biol Chem 281:21745–21754.

Ramadori G, Lee CE, Bookout AL, Lee S, Williams KW, Anderson J, Elmquist JK, Coppari R (2008) Brain SIRT1: anatomical distribution and regulation by energy availability. J Neurosci 28:9989–9996.

Raval AP, Lin HW, Dave KR, Defazio RA, Della Morte D, Kim EJ, Perez-Pinzon MA (2008) Resveratrol and ischemic preconditioning in the brain. Curr Med Chem 15:1545–1551.

Renthal W, Kumar A, Xiao G, Wilkinson M, Covington HE 3rd, Maze I, Sikder D, Robison AJ, LaPlant Q, Dietz DM, Russo SJ, Vialou V, Chakravarty S, Kodadek TJ, Stack A, Kabbaj M, Nestler EJ (2009) Genome-wide analysis of chromatin regulation by cocaine reveals a role for Sirtuins. Neuron 62:335–348.

Roth GS, Ingram DK, Lane MA (1995) Slowing aging by calorie restriction. Nat Med 1:414–415.

Selcher JC, Atkins CM, Trzaskos JM, Paylor R, Sweatt JD (1999) A necessity for MAP kinase activation in mammalian spatial learning. Learn Mem 6:478–490.

Trejo JL, Piriz J, Llorens-Martin MV, Fernandez AM, Bolós M, LeRoith D, Nuñez A, Torres-Aleman I (2007) Central actions of liver-derived insulin-like growth factor I underlying its pro-cognitive effects. Mol Psychiatry 12:1118–1128.

Trifilieff P, Calandreau L, Herry C, Mons N, Micheau J (2007) Biphasic ERK1/2 activation in both the hippocampus and amygdala may reveal a system consolidation of contextual fear memory. Neurobiol Learn Mem 88:424–434.

Tronche F, Kellendonk C, Kretz O, Gass P, Anlag K, Orban PC, Bock R, Klein R, Schütz G (1999) Disruption of the glucocorticoid receptor gene in the nervous system results in reduced anxiety. Nat Genet 23:99–103.

Valverde F (1976) Aspects of cortical organization related to the geometry of neurons with intra-cortical axons. J Neurocytol 5:509–529.

Vaquero A, Scher M, Lee D, Erdjument-Bromage H, Tempst P, Reinberg D (2004) Human SirT1 interacts with histone H1 and promotes formation of facultative heterochromatin. Mol Cell 16:93–105.

Wareski P, Vaarmann A, Choubey V, Safiulina D, Liiv J, Kuum M, Kaasik A (2009) PGC-1alpha and PGC1-beta regulate mitochondrial density in neurons. J Biol Chem 284:21379–21385.

Weindruch R, Walford RL, Fligiel S, Guthrie D (1986) The retardation of aging in mice by dietary restriction—longevity, cancer, immunity and lifetime energy—intake. J Nutr 116:641–654.

Yeung F, Hoberg JE, Ramsey CS, Keller MD, Jones DR, Frye RA, Mayo MW (2004) Modulation of NF-kappaB-dependent transcription and cell survival by the SIRT1 deacetylase. EMBO J 23:2369–2380.

Zhang J (2007) The direct involvement of SirT1 in insulin-induced insulin receptor substrate-2 tyrosine phosphorylation. J Biol Chem 282:34356–34364.

Zhao X, Sternsdorf T, Bolger TA, Evans RM, Yao TP (2005) Regulation of MEF2 by histone deacetylase 4- and SIRT1 deacetylase-mediated lysine modifications. Mol Cell Biol 25:8456–8464.

Zhou Z, Hong EJ, Cohen S, Zhao WN, Ho HY, Schmidt L, Chen WG, Lin Y, Savner E, Griffith EC, Hu L, Steen JA, Weitz CJ, Greenberg ME (2006) Brain-specific phosphorylation of MeCP2 regulates activity-dependent Bdnf transcription, dendritic growth, and spine maturation. Neuron 52:255–269.